Effects of plasma treatments of polypropylene adhesive joints used in the automotive industry

Effects of plasma treatments of polypropylene adhesive joints used in the automotive industry

R. Ciardiello[1*], D. D'Angelo[2], L. Cagna[3], A. Croce[3], D. S. Paolino[1]

[1]Department of Mechanical and Aerospace Engineering, Politecnico di Torino, Corso Duca degli Abruzzi 24, 10129 Turin, Italy

[2]Plasma Nano-Tech - Environment Park, Via Livorno 60, 10144 Turin, Italy

[3]Department of Science and Technological Innovation, University of Eastern Piedmont, Viale T. Michel 11, 15121 Alessandria, Italy

***Corresponding Author*:**
Raffaele Ciardiello
E-mail address: raffaele.ciardiello@polito.it
*Full postal address:*C.so Duca degli Abruzzi 24,
Department of Mechanical and Aerospace Engineering – Politecnico di Torino,
10129 – Turin,ITALY

Keywords: Plasma treatment, Vacuum Plasma, Atmospheric Plasma, Mechanical Properties, Ageing, Polypropylene.

Abstract

Plasma treatment has been used in recent years to activate the surfaces of adhesive substrates and thus as an adhesion promoter between adhesive and substrates. The use of plasma treatments is widely adopted in the automotive industries especially for polymers that present low surface energy, such as polypropylene. In this work, polypropylene substrates used in the automotive industries have been treated with two different techniques: vacuum and atmospheric plasma. Then, polyurethane and methacrylate adhesives have been used to bond single lap joints (SLJs). Typically, these two adhesives cannot bond polypropylene substrates without surface treatments. An experimental plan has been designed to investigate the process parameters that can increase the functional polar groups (FPG) maximising the adhesion strength. Besides the types of plasma, two different gas carriers (air and nitrogen) and different treatment times have been investigated. The substrates, treated and not treated, have been assessed through Scanning Electron Microscope (SEM) analysis, Energy Dispersive X-ray analysis (EDX) and Fourier-Transform Infrared Spectroscopy (FT-IR) to quantitatively assess the increment of FPG after the different treatments. The experimental plan shows that the atmospheric plasma can improve the surface of the substrates by using a smaller time. Mechanical tests on SLJs show that methacrylate and polyurethane cannot bond polypropylene substrates without the plasma treatment. On the other hand, the treated substrates can form a strong bonding with the adhesive since all SLJs exhibit a substrate failure. Mechanical tests have been also carried out after three different ageing cycles showing that the adopted plasma treatment is not affected by the ageing cycles.

1. Introduction

In recent years, the automotive industry is moving towards the usage of lighter and more sustainable materials such as thermoplastic polymers and composite materials [1]. Vehicle lightening is a direct consequence of the need to reduce fuel consumption and environmental pollution or increase the life cycle of batteries for hybrid and electric vehicles. Indeed, it has been demonstrated that by reducing the vehicle weight of 100 kg, CO_2 emissions may reduce up to 8 g/km depending on the vehicle size and powertrain type [2].

The adoption of lightweight materials leads to the necessity of finding more efficient joining techniques. Adhesive joints represent a good substitute for the traditional mechanical fasteners for different reasons. They represent the most promising alternative when bonding different materials or hybrid structures (i.e. composite/plastic joints) [1] since they do not need holes or drilled parts that induce discontinuity in the structures [3]. Furthermore, they ease the manufacturing processes, they have sealant properties, and some of them can also resist to corrosive environments [4]. Despite these advantages, for some materials, such as polypropylene (PP), the bonding process has some criticalities that may limit the diffusion of adhesive joints, in particular in the industrial field. To cope with these criticalities, some techniques are typically used to improve the adhesion properties of the substrates such as flame, plasma or laser treatment that can improve the surface properties of the components enabling the adhesive bonding. Among these, plasma treatment is reported as one of the most effective techniques to activate the substrate surfaces of different materials with long-term durability [5-6].

Gas plasmas are ionized gases formed by liberating electrons from gas molecules and atoms using high electrical voltages. Plasma exposure can modify the surfaces of the polymer producing highly reactive zones (surface activation). Further, it can clean the surfaces from contaminants and can be used for etching processes [7-8]. It is possible to obtain different mixtures of ions, radicals and FPG, depending on the gas used, which may modify in different ways the surface properties of the treated samples. The activation of the polymer surfaces may significantly improve the adhesion performance and increases its hydrophilicity, which is another beneficial effect for the adhesion. The most used plasma systems are vacuum and atmospheric plasma. Vacuum plasma systems (VPS) allow controlling the process in a vacuum chamber by using only the gasses that must be ionized [8]. The main advantages of this plasma system are that it can completely control the atmosphere of the process and it can treat together different components or specimens based on the size of the chamber. On the other hand, atmospheric plasma systems (APS) work in the ambient air and plasma species coming out from the source get in contact with the elements present in the air. Thus, the plasma can react with the elements that are present in the environment. The main advantage of APS is the simplified treatment system that does not need a special chamber and is performed directly on the surface to be treated. For this reason, many industries, in particular automotive industries, prefer APS since it can be directly oriented on the surfaces that have to be treated before bonding the components. The cold APS jet is one of the most used since it can be easily adopted for on-line industrial applications. Further, it has a large number of operational parameters (process gas composition, working distance of the jet, electrical power and treatment time) which can be adjusted to achieve the best adhesion results [5-6].

In the last years, the use of plastics and composite materials has significantly increased in the automotive industry, and this is leading to the adoption of adhesives for bonding several components also made of different materials. For this reason, many works have been carried out to improve the adhesion properties between substrate and adhesives taking into account different methods. Sarac et al. [9] used Al_2O_3 nanoparticles to increase the mechanical properties and the failure surfaces, switching from adhesive to adhesive/cohesive failures. Adin et al. [10, 11] and Kurtkan et al. [12] showed different strategies to increase the mechanical properties of an adhesive joint by modifying the sizes of the substrates (thickness and width) and the bonding area. Kurtkan et al [12] showed that the bonding area can be designed to increase the mechanical performance of the adhesive joints by adding rivets to the adhesive joints.

Although some of these strategies can be adopted for many materials, PP substrates are difficult to bond and many papers show that it is difficult to obtain a cohesive failure [13]. PP is extensively used in the automotive sector (e.g., for dashboards, home lamps, plastic bumpers and as skins of some door panels) because it is

cheap, with good mechanical properties and good chemical resistance [14]. However, PP is a material that exhibits a hydrophobic behaviour because of its low surface energy that makes this material very hard to bond [1, 14]. One of the main problems related to the surface of PP substrates is the lack of oxygen-based FPG. Plasma treatments can improve these polar surfaces by increasing the concentration of FPGs on the polymer surface [7,15]. These oxygen radicals react with carbon atoms on the PP surface more readily than oxygen molecules, thus forming a larger number of oxygen-based FPGs. The heat generated by the plasma source also induces a thermal oxidation effect. This effect facilitates the abstraction of hydrogen atoms from the surface PP units (CH_2=CH–CH_3), as in the case of UV-induced oxidation [15,16]. These kinds of polymeric radicals can react with oxygen radicals and ions to a greater extent contributing to increase the amount of oxygen-based FPGs.

Many works [17-23] showed the surface modification of the PP by using VPS and APS. Mü Hlhan et al. [23] performed VPS treatments using pure oxygen as a process gas for polypropylene substrates to increase the adhesion with a cyanoacrylate-based adhesive. They found that the plasma treatment is more effective with a short exposure time. Green et al. [22] studied the effect of VPS and APS treatments on PP substrates considering the modification of the O:C ratio on the surface. Further, they studied how this aspect can influence the adhesion properties with a polyurethane adhesive. APS treatment showed a lower O:C ratio and higher roughness. They also noticed that a higher O:C ratio leads to higher shear strengths of the bonded joint. On the other hand, Bhattacharya et al. [24] used a different approach that takes into account the contact angle. They reported that contact angle is strongly correlated to the bond strength of polymer materials. Although the effect of treatment time has been analysed in different studies maintaining constant both gas mixture and working distance (WD), Bhattacharya et al. [24] showed that there is a direct dependency between the contact angle and the mechanical strength. Lower contact angles increase the wettability of the surface and thus the mechanical strength of the joints [24]. Keher et al. [5] observed that both peel strength and surface free energy of PP surfaces can significantly increase in the case of small WD with APS in air and nitrogen. The maximum peel force values, which correspond to cohesive failure of the adhesive joints, is obtained for WDs between 4 mm and 8 mm and it reaches higher values in the case of nitrogen plasma [7]. This behaviour can be explained by the fact that nitrogen plasma in atmospheric conditions produces a higher concentration of water-soluble low-molecular-weight oxidized materials (due to higher deposition of carboxyl functional groups) which increases the surface energy of the substrate [7, 17]. Another operational parameter that has a high influence on the adhesion is the radio frequency (RF) power setting. It was found [25,26] that, by increasing the plasma RF power in atmospheric conditions, the contact angle greatly decreases and the surface energy significantly decreases.

In this work, polyurethane and methacrylate adhesives are used to bond plasma-treated PP substrates since these adhesives cannot adhesively bond PP. APS and VPS have been used for treating PP substrates used in the automotive industry and studying the effects of the plasma on the surfaces. Further, the mechanical behaviour of adhesive joints before and after ageing cycles has been analysed. The methodology proposed in this work aims to preliminarily identify qualitatively and quantitatively the effect of VPS and APS by assessing the variation of the oxygen percentages on the treated surfaces compared to the untreated samples. Then, the treatment that led to the largest increase of oxygen, APS with air and nitrogen, were further evaluated by studying the effect of the treatments on the contact angles and surface tension to verify whether the modifications were effective. Finally, SLJ tests were carried out before and after ageing cycles currently adopted by automotive industries. The methodology proposed in this work that uses the same approach with two different adhesives, to the best of the authors' knowledge, has not been presented in literature before.

2. Materials and methods

The material for the substrates is provided by LyondellBasell (Hostacom CR 1171 G1A). The material is a polypropylene (PP) copolymer filled with 10% of talc, largely used in the automotive industry for different

components (i.e. plastic bumpers, dashboards, home lamps and different skins) [14]. Rectangular adherends, 100 mm long with cross-section 20x3 mm, were used as substrates for the experimental tests. A polyurethane and a methacrylate adhesives, used in the automotive industry, are used to bond the PP substrates before and after the plasma treatments. The polyurethane adhesive is a two-component adhesive (Isocyanate-Polyol) provided by DOW Automotive Systems (BETAFORCE 2850L). The mixing ratio (resin-hardener) is 1:1 and it is mainly designed for composite materials and painted metals [9]. The methacrylate adhesive, provided by Plexus (MA920), is a two-component methacrylate adhesive designed for structural bonding. The mixing ratio (resin-hardener) is 10:1 and it is mainly designed for composite materials and metals. The main properties of the polyurethane and methacrylate adhesives are reported in Table 1.

Table 1: Main properties of the two investigated adhesives [27, 28]

	Polyurethane adhesive	**Methacrylate adhesive**
Viscosity [Pa*s]	30*	75
Glass transition temperature [°C]	-45	125
Open time [min]	35-50	4-6
Density [g/cm^3]	1.3	0.97
Tensile strength [MPa]	10	13
Elongation at break [%]	150	90
E-Modulus [MPa]	21	600
Curing time	24 h	16 min

* Extrusion, Ballan 4bar, 2mm nozzle [g/min]

Plasma treatments are carried out with two different systems. The first system is a low-pressure VPS treatment by Diener electronic GmbH. The system model is PICO. This system uses a power of 200 W and it works in a vacuum chamber that avoids the influence of contaminants or the interaction with the environment. The second system is an APS that is a plasma jet system from Plasmatreat GmbH (Steinhagen, Germany) model Openair-Plasma®. In this case, the plasma gas coming out of the jet system is in contact with the atmosphere. Therefore, different FPG can be found on the treated surface due to the interaction of the plasma with the air. Thus different constituents can be found on the treated surface even if a specific gas carrier is used [10]. During the plasma treatment, the PP temperature does not overcome 120°C, which is quite below the softening temperature of the PP substrates (160°C).

The APS works with an input pressure of 5.0 bar and a flow rate of 30 l/min. A computerized numerical control system can move the torch on the specimens along two axes at a fixed distance from the surface. A linear velocity of 100 mm/sec was used to move the torch along the longitudinal direction of the sample to treat the specimens in the bonding area. 5, 10 and 15 translations of respectively 5, 10 and 15s were set up to treat the specimens. The treatment times were chosen based on the results reported in Section 3.3. However, although the entire process durations are 5, 10 and 15s, the exposure times are much lower, 1.25, 2.5 and 3.75s respectively. These are the exposure times related to the passage of the torch on the bonding area (25 mm long). The APS treatments were carried out at a power of 600 W. The working distance between the nozzle and the substrate was kept constant at 8 mm. The excitation frequency for the plasma is 25 kHz. The generator delivers a pulse-pause modulated current. The current modulation is controlled by adjusting the plasma cycle time (PCT). With a PCT of 100%, the pulse duration is equal to the pause duration [29]. The parameters for the APS process are shown and summarised in Table 2. This last reports also the contact angles and the surface tensions that were measured on the PP substrates. As reported also in other works [21,22,24], the contact angle decreases with the exposure time while the surface tension increases for both

air and nitrogen APS. Table 2 reports an increase of surface tension after 3.75s that is around 180% compared to the untreated specimens. On the other hand, the contact angle decreases by 2.5 times (assessed with water) and 1.6 times (assessed with CH_2I_2) in the case of APS with nitrogen and of respectively 2.7 and 1.5 times.

Table 2: Process parameters of the APS system.

Treatment	PCT	Number translations	Exposure time	Contact angle		Surface tension
		-	s	Polar (Water)	Apolar (CH_2I_2)	mN/m
Untreated	-	-	-	93.3	78.2	22.4
Air	100	5	1.25	71.5	68.6	39.5
Air	100	10	2.5	51.9	55.0	53.2
Air	100	15	3.75	38.2	49.2	62.3
Nitrogen	90	5	1.25	72.1	68.5	37.4
Nitrogen	90	10	2.5	50.1	58.7	53.2
Nitrogen	90	15	3.75	34.1	51.8	63.9

Both VPS and APS treatments were carried out with two different gas carriers, air and nitrogen. The experimental plan is developed in three different phases. First, a complete characterisation of the untreated sample is carried out. Then, VPS and APS are adopted by using nitrogen and air in the second part of the analysis to define the treatment effectiveness. The treatment times (5, 10 and 15 min) for the VPS and (5, 10 and 15 s) for the APS, are chosen based on the results of previous works [21,22, 24,29] and based on the results presented in section 3.3. The objective was to minimise the contact angle and increase the hydrophilicity of the samples. The treatment times between APS and VPS are quite different due to the different mechanisms that APS and VPS use. VPS uses a gas that is ionized in a vacuum chamber to form plasma and a power of 200W. On the other hand, APS system uses a plasma jet close to the surface to treat and it works at an approximate pressure close to the surrounding atmosphere. The APS uses a power of 600W. Furthermore, Shibada et al. [30] and Shutze et al. [31] showed the effect of pressure on the composition of plasma based on Shibata's model [31]. They found that the concentrations of ions and atoms are lower in a VPS than those in APS.

Nevertheless, the impingement rate of these species on the substrate may be about the same in both cases. This is because the flux to the surface increases with the decrease of pressure and with the increase of exposure time [30]. In contrast, their studies [30] show that, at atmospheric pressure, ions will be quite irrelevant, consequently the chemistry will be dominated by relatively neutral species. The spectra acquired and shown in Section 3.3 indicate that radical species (N and O atoms) exist at high densities in the plasma jet source (APS). Previous works [21,22,24,29] studied the effects of the treatment times with APS and VPS systems with respect to the contact angles and surface tensions. These works reported that VPS systems need higher time to obtain a decrease of the contact angles and an increase of the surface tensions compared to APS systems.

These preliminary analyses show that the APS with the nitrogen gas carrier leads to a significant increase of the oxygen percentage and, for this reason, APS with nitrogen is chosen to treat the specimens. The effect of the treatment time is evaluated with APS and nitrogen at three levels: 5 s, 10 s and 15 s. The differences in the treatment times, 15 min for the VPS and 15 s for the APS, are due to the different systems that work with different powers and with different mechanisms. Further, the APS is directly oriented on the area to treat and uses a higher power compared to the VPS.

The assessment of the treated surfaces has been carried out with three different systems. SEM and EDX are used to evaluate any change in the substrate morphology (SEM) and the elements that are present on their surfaces (EDX). This preliminary part is mainly carried out for assessing the increase of oxygen after the plasma treatments. This is because polyurethane and methacrylate adhesives can increase their adhesion with PP substrates, if the PP surface presents oxygen-based FPGs [24]. The micro-IR analysis is finally adopted to study the variation of the oxygen-based functionalities and the increase of the degree of hydrophilia.

SEM and EDX analyses are carried out by using ESEM Quanta 200 machine (FEI Company) with EDX microprobe (EDAX). The system is set at a relatively low pressure of 90 Pa, at a working distance of 10 mm and a voltage of 20 kV. The samples are not metallised to avoid any possible contamination. Surface roughness is evaluated in SEM micrographs, using an ImageJ software plugin, denominated SurfCharJ plugin [32]. This measurement allows to calculate some parameters, such as Ra (arithmetical mean deviation), Rq (root mean square deviation), Rsk (kurtosis of the calculated profile), and Rku (skewness of the calculated profile), which are reported in Section 3.2. In this way, it was possible to evaluate the effects induced by plasma-treatments also on the roughness and to better compare the different sample surfaces.

Micro-IR analyses are performed using a Nicolet iN10 machine (Thermo Fisher Scientific Inc.), with a sampling area of 150 μm, a number of scans equal to 256, and a spectral range between 4000 and 675 cm^{-1}. However, in this paper the spectra will be shown in the range 3500 and 675cm^{-1} where lie the absorption bands of the fundamental vibrations related to the most common organic molecules.

Differential scanning calorimetry (DSC) measurements were carried out using a DSC 3 STARe System (Mettler Toledo). A heating rate of 10°C/min and a purge gas with a flow rate of 50 mL/min were applied. The sample weights were ~7 mg and alumina crucibles with not-perforated lid were utilised for the analyses.

SLJ specimens are prepared using an aluminium mould, shown in Figure 1. The lower substrates are placed on the lower base of the fixture, then, the adhesive is uniformly spread on the substrate and the upper substrate is positioned on the upper base of the fixture by applying a mass that ensures the squeezing of the adhesive excess. The system has been designed to obtain the correct overlap length by the use of pins and a correct value of the adhesive joint thickness given by the different heights of the upper and lower bases of the fixture. The overlap length used for this experimental activity is 25 ± 0.1 mm and the adhesive thickness is 1.5 ± 0.05 mm for both the polyurethane and methacrylate adhesives as suggested by the technical datasheet of the provider. SLJ tests were conducted at a constant displacement rate of 5 mm/min using an Instron 8800 hydraulic machine. At least, five bonded joints were tested for statistical purposes. The substrates were adhesively bonded after the plasma treatment procedures without any further process before bonding.

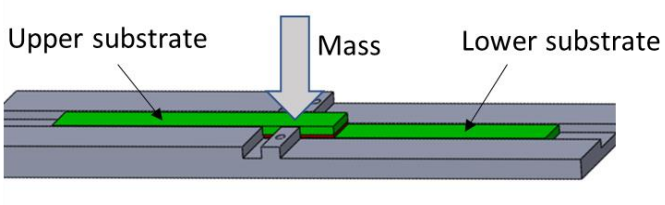

Figure 1: Fixture for the preparation of the SLJ

The mechanical properties of the adhesive joints are studied before and after three different ageing cycles. The used ageing cycles are defined by a Stellantis standard [33]. The ageing cycles are:

Cycle A: Exposure at 90 °C without the control of the Relative Humidity (RH) for 500 h.

Cycle B: Exposure at 40 °C with RH set at 98% for 500 h.

Cycle C: Exposure at 80 °C without RH for 24 hours; Exposure at 40 °C with RH set at 98% for 24 hours; Exposure at -40 °C for 24 hours.

Ageing cycles are carried out by using two different chambers (Votsch VT4020 and Votsch Heraeus HC0020) that present a maximum temperature fluctuation of ±0.3 °C.

3. Results and discussion

The SEM/EDX and FT-IR analyses are presented in this section together with the SLJ tests conducted before and after the ageing. Furthermore, the reaction mechanisms involved with the adopted plasma are presented.

3.1Characterisation of the untreated surfaces

Figure 2 shows the SEM/EDX and micro-IR analyses for the untreated specimens. These analyses represent the baseline of the experimental activity and are used to assess the effectiveness of the plasma treatments. Figure 2a depicts the surface morphology before treatment. This figure is representative of a larger area and shows that the surface morphology is quite homogeneous, except for two inhomogeneities in the surface that are displayed in Figure 2a. Figure 2b shows a table with the element found in the EDX analysis together with the relative percentages. As stated in Section 2, the element of more interest for the adhesive used in this activity is the oxygen (O) because it can increase the adhesion properties with the adopted adhesives. However, magnesium (Mg), silicon (Si), and calcium (Ca) have been reported in the analysis since Si and Mg are constituent elements of the talc and Ca of the carbonate, which are embedded in the PP substrates. Figure 2c shows the surface computed surface morphology assessed from the SEM image by the ImageJ SurfCharJ plugin [32]. Finally, Figure 2d displays the IR spectrum of the untreated specimen. This analysis is used for verifying the increase of oxygen-based functionalities and the increase in the degree of hydrophilia. The IR spectrum shows the region ranging from 3500 to 675 cm^{-1}, useful to understand whether FPGs change after the treatments.

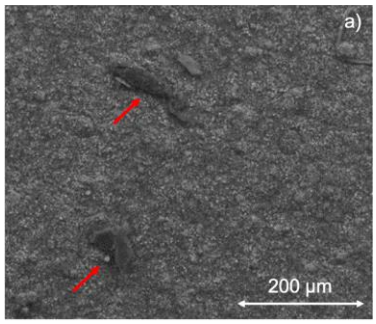

b)

Elements	At %
C	62.67
O	21.08
Mg	2.38
Si	4.41
Ca	8.58

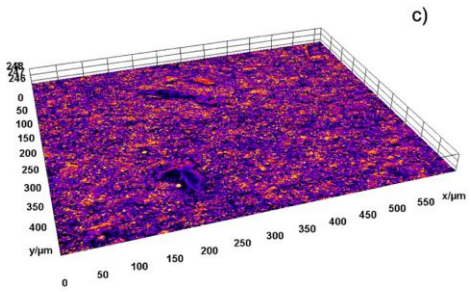

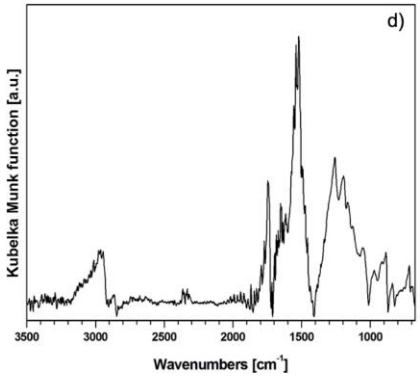

Figure 2: a) SEM; b) EDX analyses; c) 3D surface morphology obtained by SurfChar plugin; d) FT-IR spectrum of the untreated specimens

3.2Preliminary analysis

VPS and APS are adopted in this preliminary analysis to assess the effectiveness of plasma treatments on the specimens. Different treatment times, 5, 10 and 15 min for the VPS and 5, 10 and 15 s (which correspond to an exposure time of 1.25, 2.5 and 3.75s, see Table 2) for the APS are chosen based on the results of previous

works [21,22,24,29] and based on the results reported in section 3.3. Figure 3 shows the SEM analysis carried out on the surfaces that are treated by VPS and air (Figure 3a), VPS and nitrogen (Figure 3b), APS and air (Figure 3c) and APS and nitrogen (figure 3d). Figure 3 reports the SEM images related to the highest exposure times. The visual inspection of the surfaces does not show significant change after the four different treatments as can be observed by comparing the SEM images. However, these surfaces do not present inhomogeneity as shown by the untreated sample.

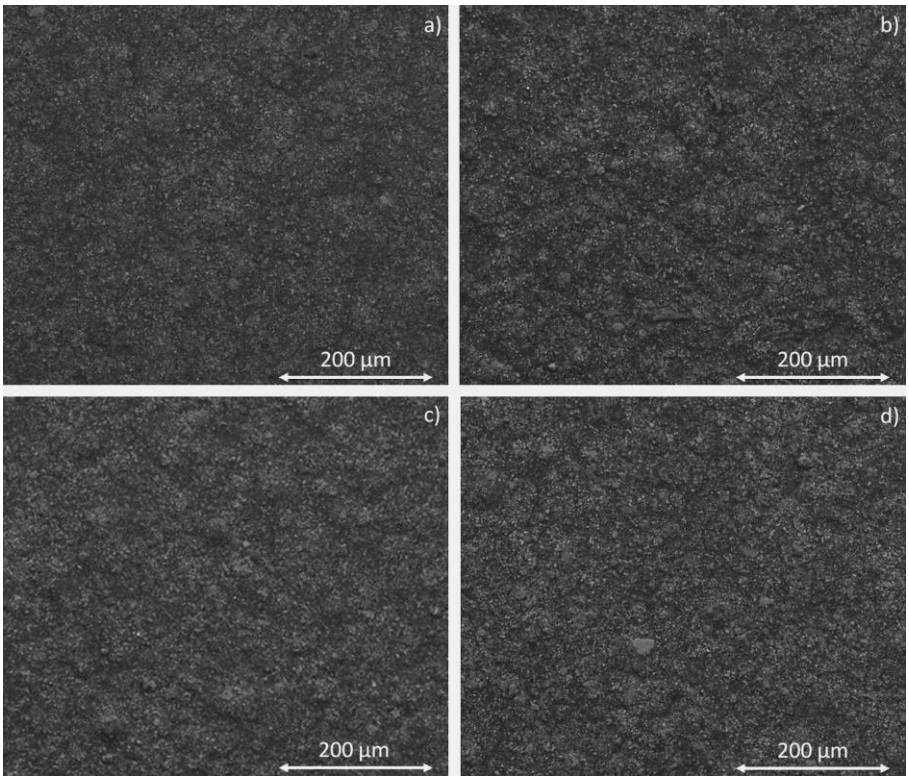

Figure 3: a) SEM image of the sample treated with VPS and air; b) SEM image of the sample treated with VPS and nitrogen; c) SEM image of the sample treated with APS and air; d) SEM image of the sample treated with APS and nitrogen

The results of the EDX analyses are reported in Table 3. The values of the standard deviations evaluated on three different points of the same specimen present a maximum error of 0.5%. The treatments with the highest exposure times are presented in Table 3 since two of them (APS with nitrogen and air) showed a significant variation of the oxygen content. This chart shows that the oxygen content does not change significantly both for the VPS that use air and nitrogen. On the other hand, the APS can significantly increase the oxygen content compared to the untreated surface, reaching an increase of 4% and 25% when air and nitrogen are used respectively. This is due to the post-plasma effect [34] that can modify the surfaces with two different mechanisms: reactions while the substrate is hit by the plasma jet, and reactions that are triggered by the plasma jet after the treatment [35]. Lommatzsch et al. [34] showed that the oxygen content can increase because of the formation of radicals on the PP surfaces that react with the oxygen present in the environment at the end of the plasma treatment.

Table 3: Chemical compositions obtained by EDX on the samples of the preliminary activity

Sample	Elements (At %)				
	C	O	Mg	Si	Ca
Untreated	62.7	21.1	2.4	4.4	8.6
Vacuum plasma-air	64.4	21.2	2.1	4.1	7.4
Vacuum plasma-nitrogen	65.8	19.9	2.1	4.0	7.4
Atmospheric plasma-air	62.9	21.8	2.4	4.3	8.0
Atmospheric plasma-nitrogen	56.3	26.3	2.8	4.9	8.9

The surface roughness of the untreated PP samples and those ones treated with APS (air and nitrogen) and VPS (air and nitrogen) after 15s and 15min respectively are reported in Figure 4 and Table 4. These results were evaluated by using SEM micrographs[32]. The micrographs of Figure 4 are computed on the SEM images of Figure 3 and are related to the PP samples treated with VPS with air after 15 min (a), VPS with nitrogen after 15min (b), APS with air after 15s (c),, and APS with nitrogen after 15s (d). Ra, Rq, Rsk and Rku parameters obtained from the images are reported in Table 4. In this way, it was possible to estimate the roughnesses of the samples to compare the different surfaces.

Table 4: Ra (arithmetical mean deviation), Rq (root mean square deviation), Rsk (kurtosis of the calculated profile), and Rku (skewness of the calculated profile) of the untreated and the treated samples

Sample	Ra	Rq	Rsk	Rku
Untreated	33.46	43.05	1.13	1.35
Vacuum plasma-air	32.44	41.74	1.14	1.30
Vacuum plasma-nitrogen	32.75	42.47	1.30	1.75
Atmospheric plasma-air	32.89	42.25	1.47	1.36
Atmospheric plasma-nitrogen	35.71	45.10	1.05	0.86

Table 4 and Figure 4 show that the quantified roughness is slightly reduced compared to untreated PP samples in the case of VPS (both air and nitrogen) and APS with air. On the other hand, it is increased for the treatment carried out using APS with nitrogen. The presence of oxygen mixed with nitrogen, which is reported in Section 3.3, probably generates new reaction channels provoking a smaller efficacy in the bombardment, due to the recombination reactions inside the plasma (NOx species creation).

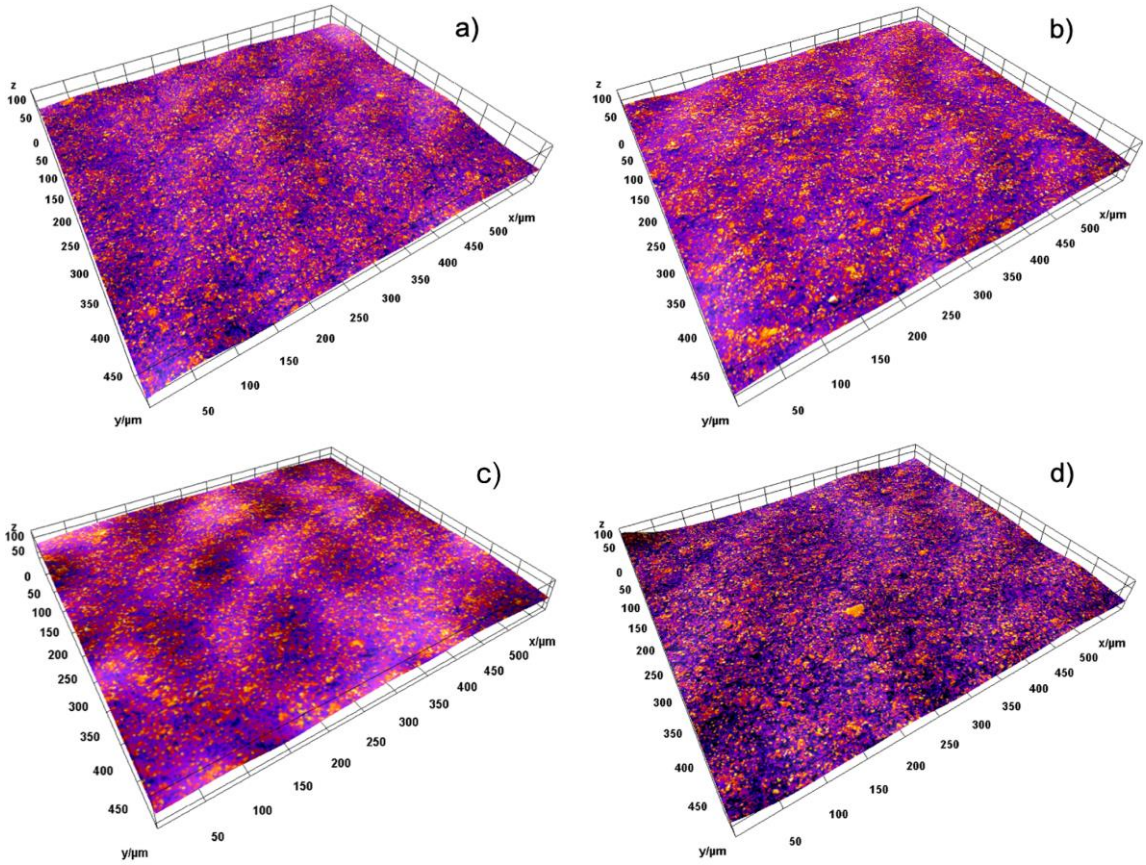

Figure 4: Surface roughness of the PP substrates treated with: a) VPS with air; b) VPS with nitrogen; c) APS with air; d) APS with nitrogen.

Figure 5 shows the micro-IR spectra of the surfaces treated with the different conditions: a) VPS with air (5, 10 and 15 min); b) VPS with nitrogen (5, 10 and 15 min); c) APS with air (5, 10 and 15 s); d) APS with nitrogen (5, 10 and 15 s). This analysis permits to assess the increase of the FPG and to evaluate whether the hydrophilicity of the surfaces increased. Figures 5a and 5b do not show significant differences compared to the untreated surface. Only a very slight increase in the OH FPG (1380 – 1420 cm^{-1}) is observed. Figure 5c shows a slight increase in functionality C=O (1647, 1747 cm^{-1}). Further, it reports an increase of the signal at 1100 cm^{-1} that is typical of the functionality C-O, and one less marked at 1380 – 1420 cm^{-1} that is typical for OH, probably associated with functionalities C-OH (alcohols). On the other hand, there is no increase of the signals at 3200 cm^{-1}, characteristic of the hydroxyl groups OH which is an index of the hydrophilicity of the system. Figure 5d illustrates an increase in functionality C=O (1647, 1747 cm^{-1}), and functionality C-O given by the increase of the signal at 1100 cm^{-1}. Moreover, there is an increase of the signal at 1380 – 1420 cm^{-1} that is characteristic of the bonds C-OH (alcohols). This evidence is also supported by the increase of the signal at 3200 cm^{-1} that is a characteristic of the hydroxyl groups OH. This improvement of O-based FPG leads to a significant enhancement in adhesion to these polymer surfaces. With oxygen or nitrogen added to the plasma activation process, polymers receive new surface functionalities particularly compatible with adhesive reactive groups.

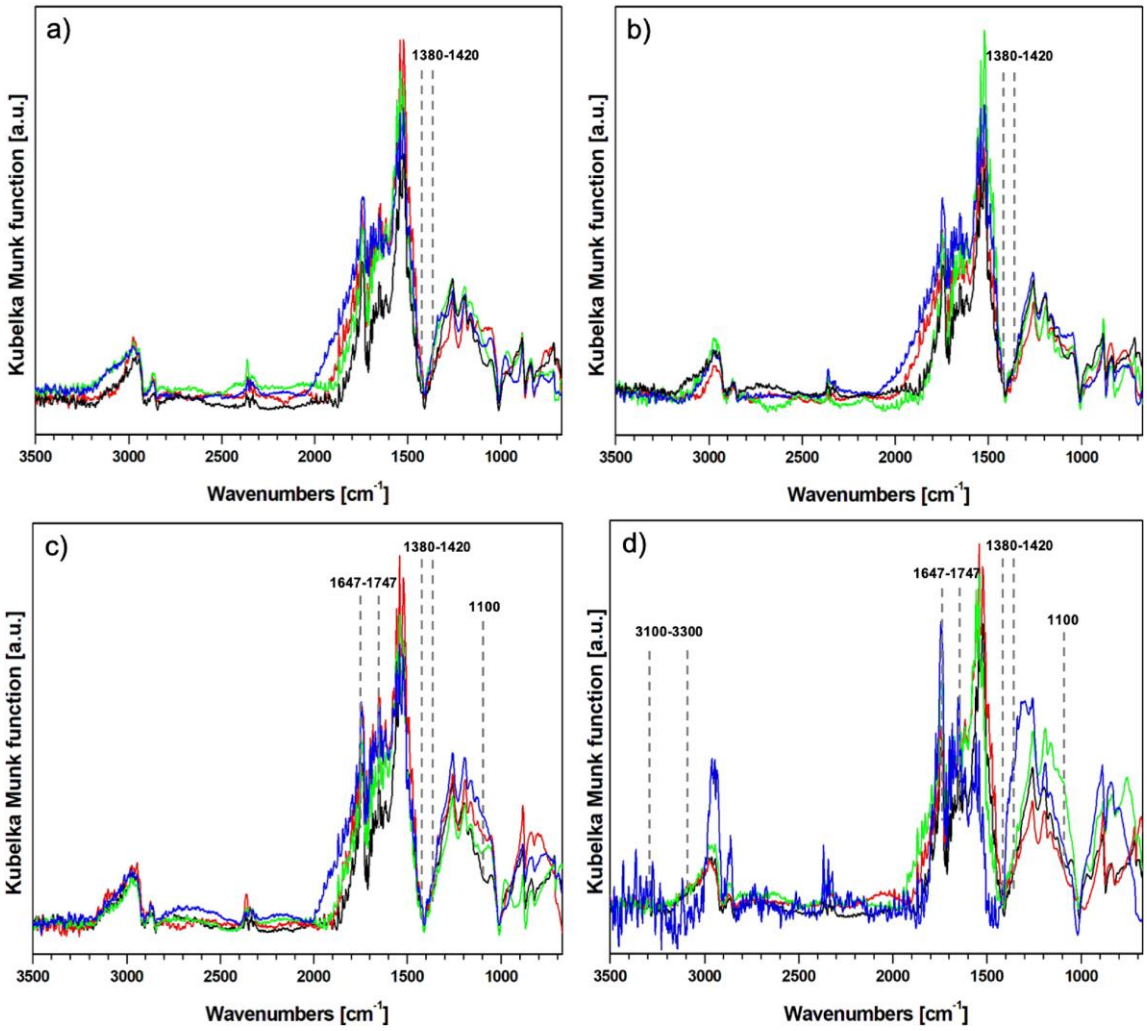

Figure 5: a) VPS with air; b) VPS with nitrogen; c) APS with air; d) APS with nitrogen. Black lines indicate raw PP, while red, green and blue ones indicate 5, 10, and 15 min treatments respectively for VPS whereas 5, 10, and 15 sec for APS

The APS treatment that uses nitrogen yields the best results with regards to the increase of hydroxyl groups and oxygen percentages. For this reason, the effect of the treatment times is also evaluated to assess the dependency of oxygen on the exposure time. The SEM analyses, Figure 6, show that there is no significant difference in the morphology of the three different surfaces as shown also in Figure 3. The three surfaces appear quite homogeneous.

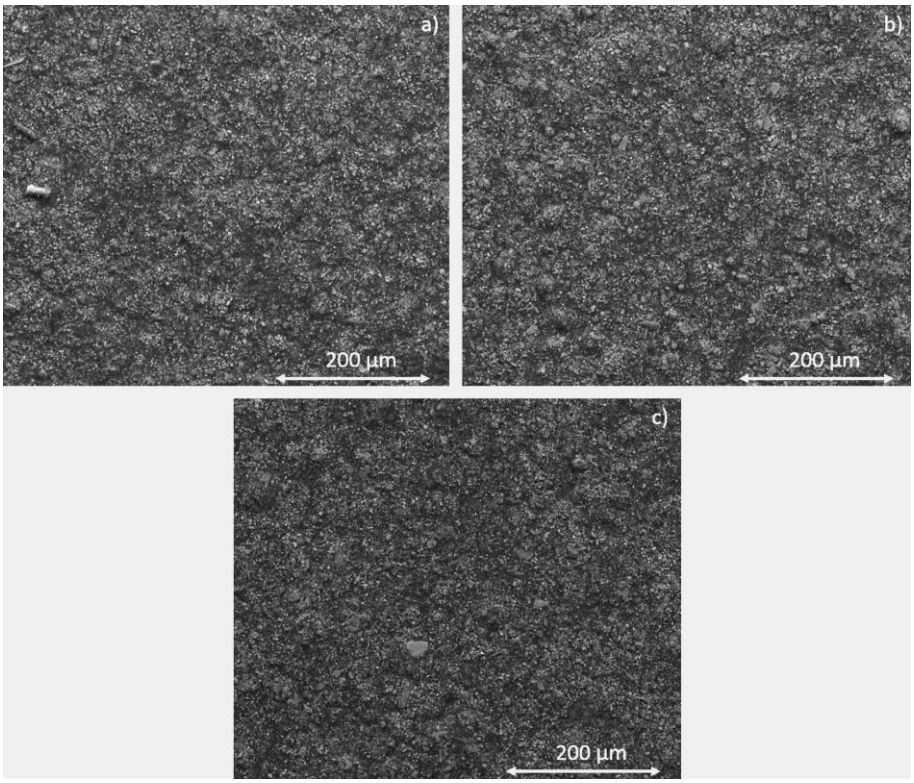

Figure 6: SEM analysis on the surfaces at different time exposure: a) 5s, b) 10s and c) 15s

Table 5 reports the results related to the EDX analyses. The chart shows that the oxygen increases with the exposure time with a close linear trend. However, a quite larger increase is shown with the treatment time of 15 s (exposure time 3.75 s). The values of the standard deviations are not reported in the table and a maximum error of 0.5% has been found.

Table 5: Chemical compositions obtained by EDX on the samples treated with APS and nitrogen

Sample	Elements (At %)				
	C	O	Mg	Si	Ca
Untreated	62.7	21.1	2.4	4.4	8.6
Atmospheric plasma-nitrogen 5s	65.1	19.9	2.1	4.1	7.9
Atmospheric plasma-nitrogen 10s	59.2	24.2	2.7	4.8	8.4
Atmospheric plasma-nitrogen 15s	56.3	26.3	2.8	4.9	8.9

The oxygen increase reported in Table 5 can be also observed in the micro-IR spectra, (Figure 7) that report an increase of C=O groups (1647 cm^{-1}, 1747 cm^{-1}), C-O groups at 1100 cm^{-1}, alcohols at 1380-1420cm^{-1} and hydroxyl groups OH. Thus, the increase of oxygen, together with the increase of the surface tension and the decrease of the contact angles were used to decide the final treatment time to adopt for the experimental campaign. APS with nitrogen and an exposure time of 3.75s was chosen to treat the PP samples for assessing the mechanical properties.

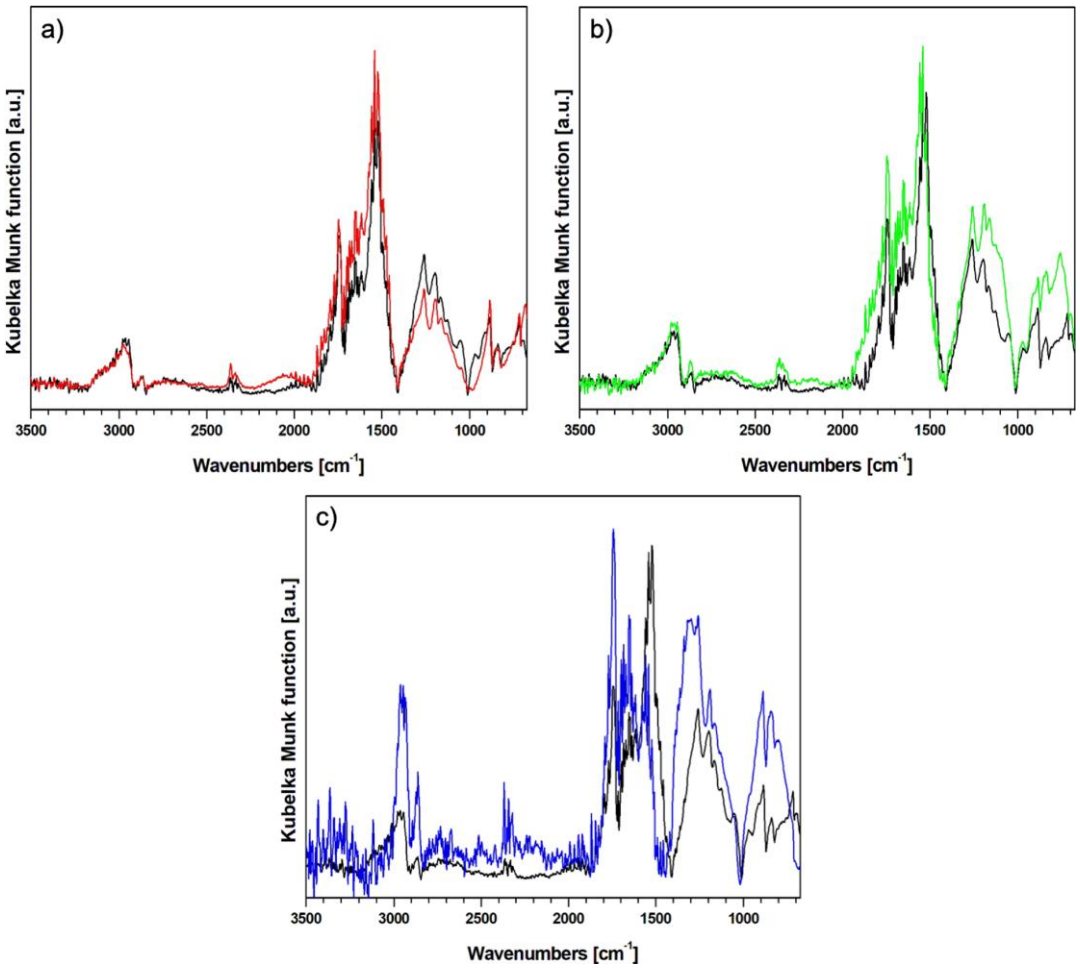

Figure 7: Micro-IR spectra of the surfaces treated with APS and gas nitrogen for different times: a) 5s; b) 10s; c) 15s

3.3 Plasma reaction related to the APS system

The reaction mechanisms that are involved with all the systems adopted in this work are reported in this section. The surface of PP polymer is formed by a basic repetitive unit of hydrocarbons. This characteristic gives hydrophobic properties such as poor wettability, adhesion and printability, especially when binding with a polar polymer using polar adhesive [36]. The difference in free energy from the surface at the interface between two polymers is quite large, so there are some problems of poor adhesion and easy detachment. Many studies [21,22,24,29] have been carried out to overcome these problems with the use of plasma treatments.

Plasma treatments can break the covalent bond by the collision of the free radicals and the electrons created in the plasma with the surface of the material. The free radicals produced on the surface of the material can combine with oxygen and moisture present in the air (or nitrogen) to form the desired surface functional groups. This work aims to induce polar functional groups to increase wettability and free energy from the surface, favouring the adhesion with polar adhesives. Thus, the evolution of the species in the plasma region, as well as the change in surface free energy and the morphology of the PP polymer were observed with regards to the different conditions of plasma treatment (vacuum vs atmospheric) in the previous Sections. The parameters of plasma treatment were treatment time and treatment power and gas mixture.

Reactions with free radicals in the gas phase led to a modification of the plasma surface of PP in a mainly oxidative way. In comparison, reactions involving gas-phase ions can be overlooked [34]. Plasma processes were characterized with optical emission spectrometry (OES) to study more accurately the origin of oxygen uptake for the nitrogen plasma treated sample.

Optical emission spectroscopy (OES) was performed by means of an Ocean Optic spectrometer LIBS2500 2plus-optic probe QP600-2-SR/BX, using integration times (optical scan) of 100 ms.

Figure 8 presents the optical afterglow spectra (OES) of nitrogen and air obtained for APS and VPS systems with air and nitrogen. The spectra confirm what is shown in the literature [35,37]. The spectrum of the air plasma, Figure 8a, is dominated by bands of NO (NOγ system, λ = 200 – 290 nm), N_2 molecules (second positive system SPS, λ = 290 – 410 nm), N_2 molecules (first positive system FPS, λ = 520 – 900 nm), and excited O atoms (λ = 777 – 844 nm).

On the other hand, in the case of N_2 plasma, Figure 8b, intense OES peaks are observed in the range of 316-466 nm and 520 – 900 nm, attributable respectively to the molecules N2, second positive system (SPS), and N_2 molecules, first positive system (FPS). Both oxygen and derived species (NO) are not present. Electronically excited and vibrational N_2 molecules are detected by the intense molecular bands of N_2 in both spectra.

Since electronic energy between 1.7 and 3.5 eV confers greater efficacy in the vibrational excitation of N_2 by the impact of electrons, we expected that large amounts of excited vibrational states N_2 would be present in both air and N_2 discharge. The effective surface activation and the incorporation of new N-containing functional groups at polymer surface are strictly correlated to the generation of both vibrational and electronically excited molecules state of N_2 and the subsequent generation of N atoms. Figures 8c and 8d show the spectra acquired by using VPS with air and nitrogen. In the first case (air discharge), in addition to the emission corresponding to N_2^+ first negative system and N_2 second positive system, the signals corresponding to an NO system at 247 nm, and two additional lines referred to excited O atoms (λ = 777 – 844 nm) are present. In the second case (pure nitrogen discharge), the main contribution to emission corresponds to the N_2 second positive system (2+) and the N_2+ first negative system (1-). Peaks representative of the N_2 second positive system (315.9, 336.7, 357.6, 380.8 nm) and the N_2^+ first negative system (391.1, 427.8, and 470.9 nm) are observed.

The combination of the spectroscopic results and the surface analysis data evidence:

1) plasma species electronically excited (N_2, N, O, NO) obtained with air plasma treatment causes modification to the PP surface;
2) that the nitrogen plasma treatment operates in absence of oxygen species in plasma afterglow.

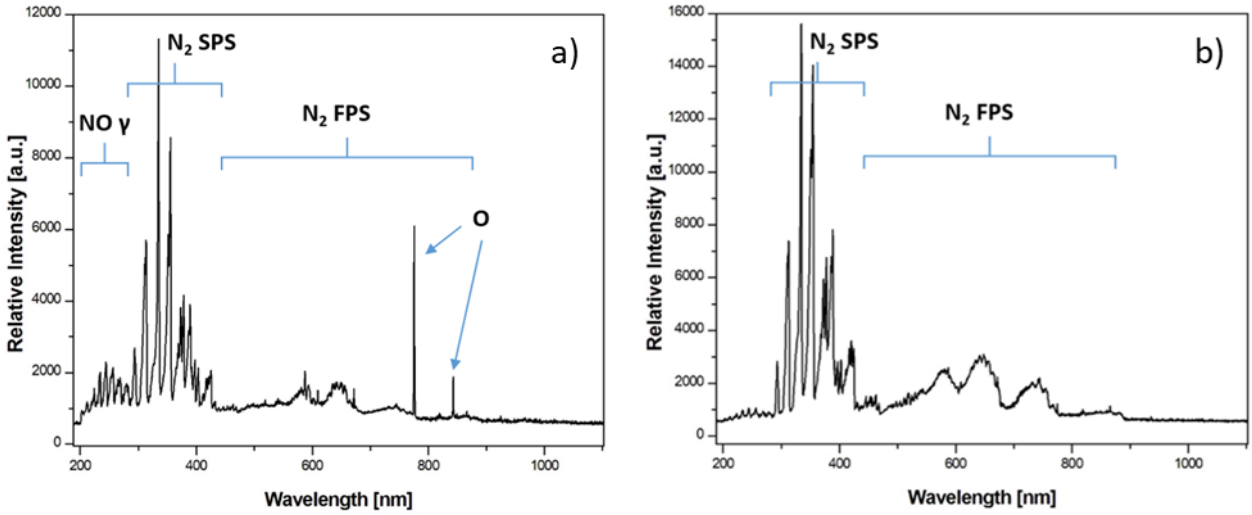

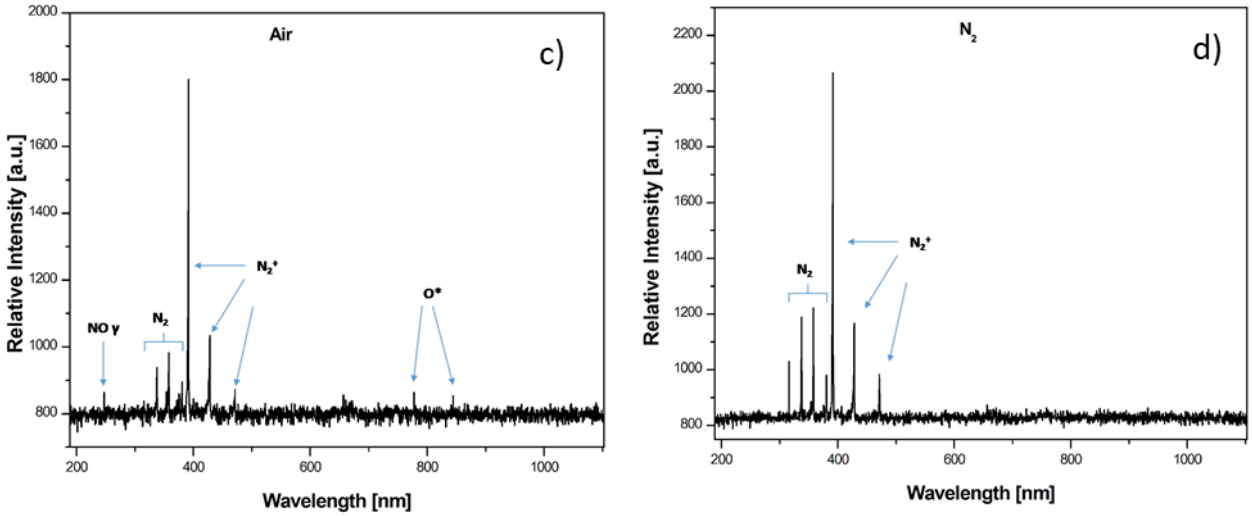

Figure 8: OES spectra for APS system: a) air and b) nitrogen; OES spectra for VPS system: c) air and d) nitrogen

The abstractions of hydrogen from the PP chain are the starting reactions [38]. The cleavage of PP at the C–C bond is possible but the resulting radicals quickly recombine to yield back the polymer. O^*_2, O_3, H, N, HO_2, O, and OH are the species in the plasma afterglow that can react with PP.

H can be abstracted from any of the primary, secondary, and tertiary sites in PP and the probability of abstraction scales ($H_{tert} > H_{sec} > H_{pri}$) in a generally independent way of the nature of the attacking radical. Some observations led to see that oxidative attack in atactic PP at tertiary sites is ≈20 times faster than at secondary sites.

Some studies have shown that O^*_2 reactions on saturated hydrocarbons are very slow [39]. The rate constant of O_3 reactivity on PP is smaller compared to both the rate constant of the gas phase consumption of O_3 and the reaction of O or OH with PP. In the same way, the reactivities of N and HO_2 towards PP are smaller compared to those of O and OH and thus they are not considered. OH has been spectroscopically observed during the oxidation of hydrocarbon polymers by atomic oxygen as evidence of H-abstraction. However, these are all the reaction channels that contribute to triggering the surface reactions. After initiation, the PP alkyl radicals can react with oxygen to form peroxyl radicals or with O to form alkoxy radicals. The reaction of polymer peroxyl radicals between propagation steps, based on their reaction with neighbouring tertiary radicals, takes about 5s. Decomposition of the resulting hydroperoxides leads to a variety of oxidized functional groups (alcohol, ketone, carbonyl, carboxyl). All these groups improve surface energy and wettability of PP surface.

The preliminary analyses carried out with SEM/EDS and FT-IR showed that the oxygen content increase was slightly significant with the specimens treated with APS and air (~4%) and significant with APS and nitrogen (~25%). The same analyses showed that the oxygen content did not change significatively with the use of VPS plasma with a long exposure time (15 min). For this reason, a second analysis was carried out to study the variation of surface energy with the treatment time with the APS system. The results of this analysis are shown in figure 9a (air) and 9b (nitrogen). Figure 9a shows the SFE of PP samples treated with air and its polar and nonpolar components. The analysis reports that the SFE increases almost linearly up to a treatment time of 15s (which corresponds to an exposure time for the surface of 3.75s). After 15s, the SFE is constant up to 28s then there is a slight decrease: for this reason a treatment time of 15s was chosen to maximise the adhesion.

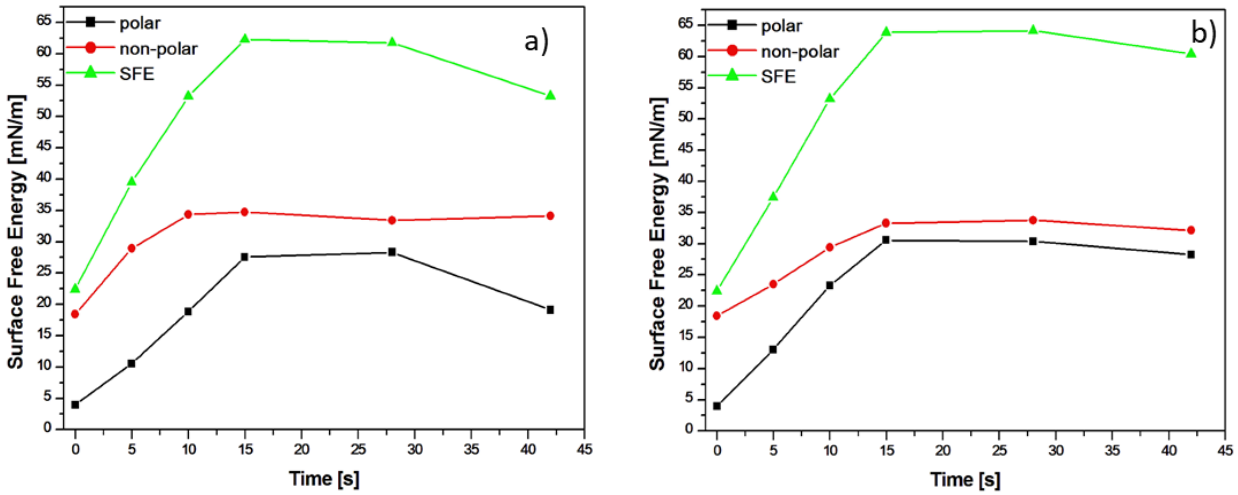

Figure 9: Surface Free Energy variation for the APS system with air (a) and Nitrogen (b)

The primary process for the formation of atomic nitrogen is the electron impact dissociation of vibrational excited N_2 states following the reaction pathway [35].

$e^- + N_2 \rightarrow N_2 (a^1 \prod_g)$; $N_2 (B^3 \prod_g)$; $N_2 (b^1 \prod_u) + e^- \rightarrow e^- + N + N$

According to these possible activation mechanisms, the nitrogen plasma treatment mainly results in N grafting on the chain terminal group giving primary and secondary amines. Therefore, the incorporation of nitrogen-containing functional groups on the surface can be explained by two steps mechanism:

1) excited nitrogen molecules in the discharge can break C-C and/or C-H bonds on the polymer surface leading to the formation of polymer radicals [40];

2) the radicals quickly react with atomic and metastable nitrogen states into the discharge, bringing to the grafting of nitrogen-containing functional groups on the polymer surface [41].

However, a consistent increase in O content is related to exposure to air[42]. This increase could be explained by the reaction of remaining free carbon-centered surface radicals (C•) after N_2 plasma treatment with ambient oxygen bringing to the formation of metastable peroxyl radicals and hydroperoxides. These lasts can decompose to stable functional groups (hydroxyl, carbonyl and carboxylic). All these functional groups lead to a significant increase in surface energy.

Comparing the processes with APS (air and pure nitrogen) it is possible to see that: a) the radical species are principally involved in the modification of the sample surface, b) the internal energy of plasma is partially employed to produce NOx compounds in the APS, c) the quantity of radical atoms N is smaller than that in pure nitrogen jet source. These may lead to the decreasing of hydrophilicity for the air plasma in comparison to nitrogen plasma.Moreover, it has been observed that getting the optical probe away from the nozzle up to 17 mm, the molecular spectral lines are clearly recorded in N_2 plasma discharge, while they decay within a few millimetres in air plasma discharge.For this reason, we have oriented our test on samples treated with pure nitrogen. In fact, eventual adoption in an industrial environment would not be affected by small variations in the management of the distance among nozzle and surface of the components to be treated.

The investigation of the variation of SFE as a function of the treatment time is shown in Figure 9b. The curves of Figure 9b show the SFE curve and its polar and nonpolar components. Also, in this case, the SFE increases up to a treatment time of 15s (which corresponds to an exposure time of 3.75s) then it is constant up to 28s and finally slightly decreases at 42s. These results obtained in Figure 9b are compatible with the increase in the signals related to the OH and C = O groups respectively to 1380-1420 cm^{-1} and 1647-1747 cm^{-1} in the IR spectra presented in Section 3.2.

3.4 Mechanical properties

The mechanical properties evaluated by means of SLJ tests are presented in Figure 10. Figures 10a and 10b report representative curves of the SLJ tests prepared respectively with the polyurethane and the methacrylate adhesives before and after ageing. The bar chart of Figure 10c shows the summary of the results carried out with both the adhesive joints prepared with the two adhesives. Finally, Figures 10d and 10e show the failure surfaces of the SLJs and the DSC analysis respectively. The curves related to unaged and aged joints prepared with the polyurethane adhesive are shown in Figure 10a. The initial trends of the curves, representative of the joint stiffness, are very similar and the curves show similar maximum force and final displacement. One criticism is related to the representative curve related to ageing cycle B that shows a slight decrease of the maximum load. The representative curves related to the methacrylate adhesive are shown in Figure 10b. They show that the initial trend and the maximum forces are quite similar for both unaged and aged specimens. On the other hand, the values of the final displacements are quite different. This is due to the temperature effect of the ageing cycles. Figure 10d shows the DSC curves relative to the polyurethane adhesive (left curve) and the methacrylate adhesive (right curve) before ageing. This analysis was carried out to assess whether there is a post-cure effect during ageing due to the high temperatures. The DSC measurements showed that while the polyurethane did not experience any thermal peak due to cure reactions, the methacrylate adhesive exhibits a peak that is starting from 47°C and ends at 85°C. Thus, the three ageing cycles enable a post-cure that leads to different mechanical behaviour.

Untreated SLJs did not bond and, for this reason, their relative SLJ tests are not reported in Figures 10a and 10b. As shown in Figure 10c, the maximum shear strengths related to the adhesive joints prepared with the polyurethane show that ageing does not affect the plasma treatment except for cycle B (wet cycle). On the other hand, the adhesive joints prepared with the methacrylate adhesive show higher strength after cycles A and C; whereas SLJs subjected to ageing B show again a lower shear strength that, however, is less noticeable compared to the polyurethane adhesive. Again, this effect could be due to the temperature effect. As shown in Figure 10e, the two adopted adhesives are not able to bond if the substrates are not plasma treated.

The untreated PP substrates were bonded with the same procedure of the treated substrates, however, there was no adhesion between the adhesive and the substrates. Indeed, many adhesive joints bonded with both polyurethane and methacrylate were separated by just removing the joints from the mould that was used to prepare the SLJ specimens. Representative failure surfaces of these adhesive joints are reported in Figure 10e.The first joint of Figure 10e is the one prepared with not treated PP and polyurethane adhesive while the second one is the representative of the joints prepared with not treated PP and methacrylate adhesive. On the other hand, the third joint in Figure 10e is representative of all the joints prepared with the treated PP. The two arrows related to the first two adhesive failures show the substrate where the adhesive remained on the surface whereas the left substrates show the adhesive failure. However, an inspection of the adhesive area showed that it is very easy to remove the adhesive from the untreated substrates. A visual inspection of the left substrates displays that there are no bonding residuals along the overlap area. Indeed, the left substrates show that there is no color discontinuity on the substrates that are indexes that there is no adhesion between substrate and adhesives. On the other hand, all the specimens prepared with the treated substrates experienced a substrate failure that is reported in Figure 10e with the third adhesive joint. The failures occurred close to the edge that is highlighted by the orange ellipse. All the substrate failures of SLJs prepared with both polyurethane and methacrylate adhesives show a similar substrate failure except for the SLJs prepared for the methacrylate adhesive and exposed to ageing cycles. These adhesive joints present higher deformations of the substrates in the area highlighted by the ellipse in Figure 10e and these larger deformations are visible in the load-displacement curves of Figure 10b.

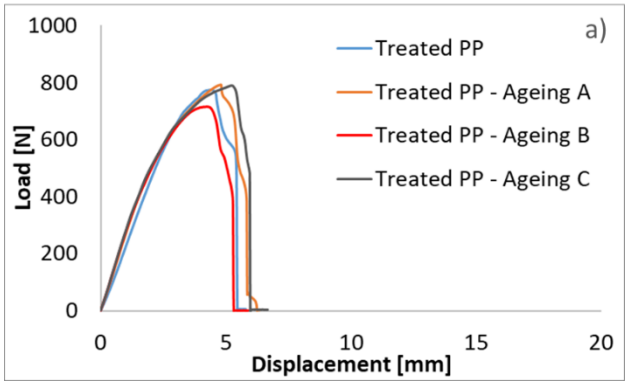

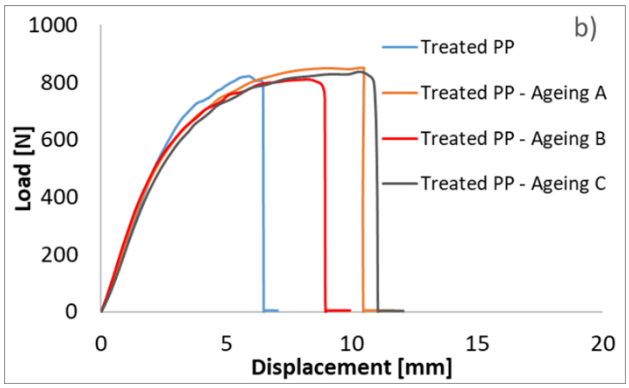

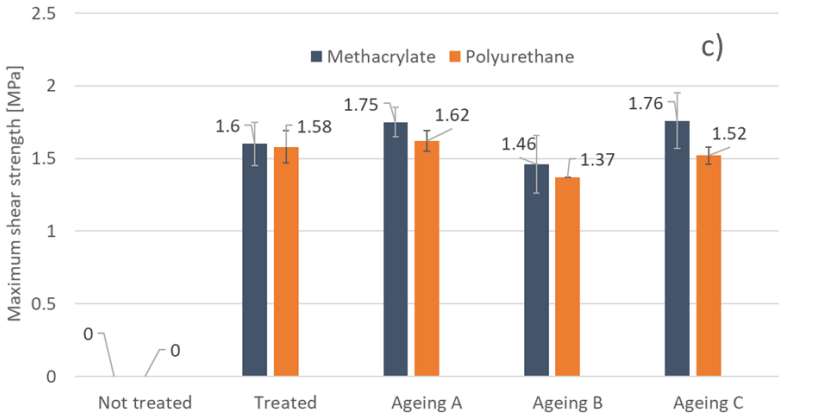

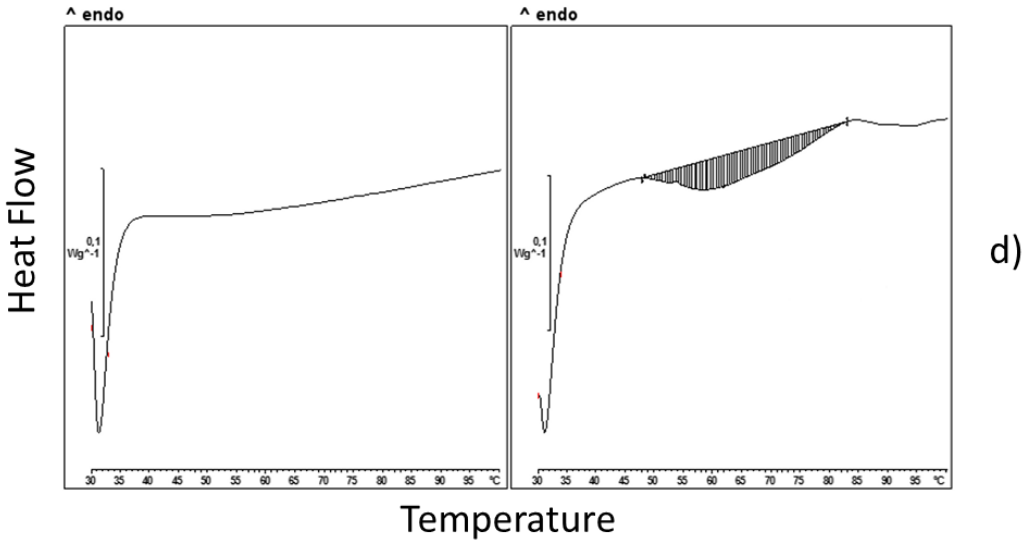

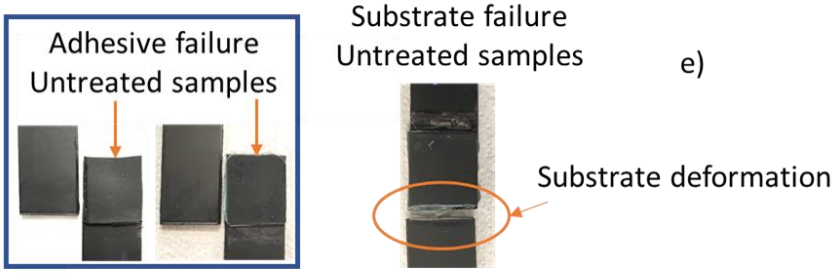

Figure 10: a) SLJ tests related to the polyurethane adhesive; b) SLJ tests related to the methacrylate adhesive; c) summary of the maximum shear strength; d) DSC analysis; e) failure surfaces

4.Conclusions

In this work, the effects of APS and VPS treatments for PP substrates have been evaluated and assessed to adhesively bond PP substrates by using polyurethane and methacrylate adhesive. The preliminary experimental activities aimed at identifying the treatment that led to the highest increase of oxygen on PP surfaces. The increase of oxygen is required to improve the adhesion between the adhesives and the substrates. The work showed that APS with nitrogen (treatment time 15s) increased the presence of oxygen by 25% compared to the untreated sample, enabling the adhesion between PP substrates and the two adhesives. FT-IR analysis showed an increase of C=O and C-O groups, alcohols and hydroxyl OH groups. The experimental activity showed that methacrylate and polyurethane adhesives were not able to bond PP substrate without plasma treatment. Further, the study showed that the selected treatment time is able to decrease the contact angle and increase the surface tension.

Although the procedure used for the untreated specimens was the same, the SLJ prepared with untreated substrates did not present adhesion since the specimens broke while they were removed from the mould. On the other hand, SLJ tests on treated (APS, nitrogen 15s) samples showed that the adhesive joints can bear relatively high loads. Indeed, all the adhesive joints tested after the treatments lead to substrate failure that is an indication of the very high adhesion between substrates and adhesives. Furthermore, SLJs have been carried out after ageing cycles. These tests showed that the ageing does not significantly affect the mechanical behaviour of the joints and that this kind of treatment can be used in the automotive industry.

Bibliography

[1] Ciardiello R, Belingardi G, Litterio F and Brunella V. Thermomechanical characterization of reinforced and dismountable thermoplastic adhesive joints activated by microwave and induction processes. Compos Struct. Epub ahead of print 31 March 2020. DOI: 101016/jcompstruct2020112314.

[2] Elmarakbi A, Ciardiello R, Tridello A, Innocente F, Martorana B, Bertocchi F, Cristiano F, Elmarakbi M and Belingardi G. Effect of graphene nanoplatelets on the impact response of a carbon fibre reinforced composite. Mater Today Commun. Epub ahead of print 14 August 2020. DOI: 01016/jmtcomm2020101530.

[3] Chang B, Shi Y and Dong S. Comparative studies on stresses in weld-bonded, spot-welded and adhesive-bonded joints. J Mater Process Technol 1999;87:230–236.

[4] Belingardi G and Chiandussi G. Stress flow in thin walled box beams obtained by adhesive bonding joining technology. Int J Adhes Adhes 2004;24:423–439.

[5] Kehrer M, Rottensteiner A, Hartl W, Duchoslav J, Thomas S and Stifter D. Cold atmospheric pressure plasma treatment for adhesion improvement on polypropylene surfaces. Surf Coat Tech 2020;403:126-138.

[6] Kostov KG, Nishime TMC, Castro AHR, Toth A and Hein LRO. Surface modification of polymeric materials by cold atmospheric plasma jet. Appl Surf Sci 2014;314:367-375.

[7] Sundriyal P, Pandey M and Bhattacharya S. Plasma-assisted surface alteration of industrial polymers for improved adhesive bonding. Int J Adhes Adhes. Epub ahead of print 15 April 2020. DOI: 101016/jijadhadh2020102626.

[8] Kusano Y. Atmospheric Pressure Plasma Processing for Polymer Adhesion: A Review. J Adhes 2014;90:755-777.

[9] Saraç I, Adin H, Temiz Ş. A research on the fatigue strength of the single-lap joint joints bonded with nanoparticle-reinforced adhesive. Weld World 2021;65:635-642. doi.org/10.1007/s40194-020-01063-2

[10] Adin H, Kılıçkap E. Strength of double-reinforced adhesive joints. Mater Test 2021;63(2):176-181.

[11] Adin H. Effect of overlap length and scarf angle on the mechanical properties of different adhesive joints subjected to tensile loads. Mater Test 2017;59(6):536-546.

[12] Kurtkan Ü, Adin H. The investigation of the tensile behaviors of single L-joint type bonded with adhesive and rivet material science and engineering technology. 2018;49(8):963-977.

[13] Ciardiello R. The mechanical performance of re-bonded and healed adhesive joints activable through induction heating systems. Mater 2021(14):6351.

[14] Belingardi G, Brunella V, Martorana B and Ciardiello R. Thermoplastic Adhesive for Automotive Applications. in Adhesives - Applications and Properties, INTECH, 2016 341-362 https://doiorg/105772/65168.

[15] Kawakami R, Yoshitani Y, Mitani K, Niibe M, Nakano Y, Azuma C and Mukai T. Effects of air-based nonequilibrium atmospheric pressure plasma jet T treatment on characteristics of polypropylene film surfaces. Appl Surf Sci. Epub ahead of print 4 December 2019. DOI: 10.1016/j.apsusc.2019.144910.

[16] Bhat NV and Upadhyay DJ. Plasma-induced surface modification and adhesion enhancement of polypropylene surface. J Appl Pol Sci 2002;86:925-936.

[17] Kehrer M, Duchoslav J, Hinterreiter A, Mehic A, Stehrer T and Stifter D. Surface functionalization of polypropylene using a cold atmospheric pressure plasma jet with gas water mixtures. Surf Coat Technol. Epub ahead of print 26 December 2019 2020. DOI: 101016/jsurfcoat2019125170.

[18] Dell'Orto EC, Vaccaro A and Riccardi C. Morphological and chemical analysis of PP film treated by Dielectric Barrier Discharge. J Phys Conf Ser 2014;550:12-15.

[19] Jones V, Strobel M and Prokosch MJ. Development of poly(propylene) surface topography during corona treatment. Plasma Process and Polym 2005;2(7):547-533.

[20] Overney RM, Lüthi R, Haefke H, Frommer J, Meyer E, Güntherodt HJ, Hild S and Fuhrmann J. An atomic force microscopy study of corona-treated polypropylene films. Appl Surf Sci 1993;64:197-203.

[21] Strobel M and Lyons CS. The role of low-molecular-weight oxidized materials in the adhesion properties of corona-treated polypropylene film. J Adhes Sci Technol 2003;17(1):15-23.

[22] Green M, Guild FJ and Adams RD. Characterisation and comparison of industrially pre-treated homopolymer polypropylene, HF 135M. Int J Adhes Adhes 2002;22:81-90.

[23] Mu Hlhan C, Weidner S, Friedrich J and Nowack H. Improvement of bonding properties of polypropylene by low-pressure plasma treatment. Surf Coat Technol 1999;119:783–787.

[24] Bhattacharya S, Datta Aberg JM and Gangopadhyay S. Studies on surface wettability of poly(dimethyl) siloxane (pdms) and glass under oxygen-plasma treatment and correlation with bond strength. J Microelectromech Syst 2005;14(3):590-597.

[25] Yoshiki H. Generation of air microplasma jet and its application to local etching of polyimide films. J Appl Phys 2006;45:5618–5623.

[26] Vishnuvarthanan M and Rajeswari N. Effect of mechanical, barrier and adhesion properties on oxygen plasma surface modified PP. Innov Food Sci Emerg Technol 2015;30:119-126.

[27] Dow Automotive Systems, “BETAFORCE™ 2850L”, Issue 2-2850L, Oct. 2013.

[28] Plexus, “TECHNICAL DATA SHEET – PLEXUS MA920”, MA920, Nov. 2017.

[29] Noeske M, Degenhardt J, Strudthoff S and Lommatzsch U. Plasma jet treatment of five polymers at atmospheric pressure: surface modifications and the relevance for adhesion. Int J Adhes Adhes 2004;24(2):171-177.

[30] Shibata M, Nakano N, Makabe T. Effect of O2(a1g) on plasma structures in oxygen radio frequency discharges. J Appl Phys 1996;80(11):6142–6147.

[31] Schungel E, Zhang Q, Iwashita S, Schulze J, Hou L, Wang Y, Czarnetzki U. Control of plasma properties in capacitively coupled oxygen discharges via the electrical asymmetry effect. J Phys D Appl Phys 2011;44:285205.

[32] Chinga G, Johnsen PO, Dougherty R, Berli EL, Walter J. Quantification of the 3D microstructures of SC surfaces. J Microsc 2007;227:254-265.

[33] Ciardiello R, Belingardi G, Martorana B and Brunella V. Effect of accelerated ageing cycles on the physical and mechanical properties of a reversible thermoplastic adhesive. J Adhes 2020;11:1003-1026.

[34] Lommatzsch U, Pasedag D, Baalmann A, Ellinghorst G and Wagner HE. Atmospheric Pressure Plasma Jet Treatment of Polyethylene Surfaces for Adhesion Improvement. Plasma Process Polym 2007;4(1):1041-1045.

[35] Tabaei P, Ghobeira R, Cools P, Rezaei F, Nikiforov A, Morent R and De Geyter N. Comparative study between in-plasma and post-plasma chemical processes occurring at the surface of UHMWPE subjected to medium pressure Ar and N2 plasma activation. Polym. Epub ahead of print 16 March 2020. DOI: 10.1016/j.polymer.2020.122383.

[36] Kwon OJ, Tang S, Myung SW, Lu N and Choi HS. Surface characteristics of polypropylene film treated by an atmospheric pressure plasma. Surf Coat Technol 2005;192:1-10.

[37] Nisticò R, Lavagna L, Boot EA, Ivanchenko P, Lorusso M, Bosia F, Pugno NM, D’Angelo D and Pavese M. Improving rubber concrete strength and toughness by plasma-induced end-of-life tire rubber surface modification. Plasma Process Polym 2021. doi.org/10.1002/ppap.202100081

[38] Dorai R and Kushner MJ. A model for plasma modification of polypropylene using atmospheric pressure discharges. J Phys D Appl Phys 2003;36:666.

[40] Massines F, Gouda G, Gherardi N, Duran M and Croquesel E. The Role of Dielectric Barrier Discharge Atmosphere and Physics on Polypropylene Surface Treatment. Plasmas Polym 2001;6:35-49.

[41] Wagner AJ, Fairbrother DH and Reniers F. A Comparison of PE Surfaces Modified by Plasma Generated Neutral Nitrogen Species and Nitrogen Ions. Plasmas Polym 2003;8:119-134.

[42] Gengenbach TR, Vasic ZR, Chatelier RC and Griesser HJ. A multi-technique study of the spontaneous oxidation of N-hexane plasma polymers.